Available online at www.sciencedirect.com
SCIENCE DIRECT®
Journal of Solid State Chemistry 178 (2005) 3014–3019
JOURNAL OF SOLID STATE CHEMISTRY
www.elsevier.com/locate/jssc

The first tin(II) vanadium(III) phosphate $SnVPO_5$: Crystal structure and magnetic properties

Roman V. Shpanchenko[a,*], Alexander S. Mitiaev[a], Victoria V. Chernaya[a], Evgeny V. Antipov[a], Hiroya Sakurai[b], Eiji Takayama-Muromachi[b]

[a]*Department of Chemistry, Moscow State University, 119992 Moscow, Russia*
[b]*NIMS, 1-1 Namiki, Tsukuba, Ibaraki 305-0044, Japan*

Received 20 May 2005; received in revised form 9 July 2005; accepted 19 July 2005
Available online 18 August 2005

Abstract

The first tin vanadium phosphate $SnVPO_5$ was synthesized by a solid-state reaction and characterized by X-ray single crystal diffraction and magnetic susceptibility measurements. The crystal structure of $SnVPO_5$ ($a = 5.2633(4)$ Å, $b = 6.5252(9)$ Å, $c = 6.8785(10)$ Å, $\alpha = 113.283(11)^\circ$, $\beta = 108.037(9)^\circ$, $\gamma = 94.603(9)^\circ$, S.G. *P*-1, $Z = 2$) is a three-dimensional framework constructed by V_2O_{10} units fasten together by tetrahedral phosphate groups. Tin atoms are situated in structure interstices. They have five-fold coordination arrangement due to a presence of sterically active lone pair which position was visualized by ELF calculations. The magnetic susceptibility shows a broad maximum at 22 K which is probably due to low-dimensional spin correlations. We propose that the magnetism of the compound can be understood by interacting spin-dimers on a distorted square lattice. Strong quantum fluctuations were suggested by unusual field dependence of the transition temperature and unexpectedly low Curie constant.

Keywords: Vanadium oxides; Tin(II) oxides; Crystal structure; Magnetic properties

1. Introduction

Vanadium containing compounds with low ($< +5$) oxidation state of V atoms attract attention of investigators since they often exhibit unusual magnetic behavior. Many compounds were reported in the Pb–V–P–O system but only three of them, namely $Pb_2(VO)(V_2P_4O_{16})$ [1], $Pb(V_2(P_2O_7)_2)$ [2] and $Pb_{1.5}V_2(PO_4)_3$ [3] contain V^{3+} cation in their structures. One would expect that close ionic radii of divalent elements should result in a formation of compounds having similar structures. The difference between ionic radii of Pb^{2+} and Sn^{2+} (1.45 and 1.36 Å for eight-fold coordination, respectively) is somewhat similar to that of Sr^{2+} (1.39 Å) and Ca^{2+} (1.32 Å). Both Pb^{2+} and Sn^{2+} cations contain sterically active lone pair. Its presence often results in strongly distorted coordination environment. Such an asymmetric environment greatly enhances the probability of appearance of technologically important properties such as piezoelectricity, ferroelectricity, nonlinear optical phenomena, and dielectric behavior.

However, up to now no information about mixed phosphates of Sn(II) and trivalent vanadium was published. The aim of the present research was the synthesis and characterization of the first tin(II) vanadium(III) phosphate, namely $SnVPO_5$, including X-ray single crystal study and magnetic properties measurements.

2. Experimental

Powder sample of $SnVPO_5$ was prepared by the solid state reaction between V_2O_3, SnP_2O_7 and metallic tin in

*Corresponding author. Fax: +7 095 939 47 88.
E-mail address: shpanchenko@icr.chem.msu.ru (R.V. Shpanchenko).

0022-4596/$ - see front matter © 2005 Elsevier Inc. All rights reserved.
doi:10.1016/j.jssc.2005.07.014

molar ratio 1:1:1. Initial mixture was pressed into a pellet, put in a corundum crucible and placed in an evacuated and sealed quartz tube. The temperature was slowly (about 10 h) increased to 700 °C. The sample was annealed at this temperature for 6 days with two intermediate grindings. The resulted bulk sample of $SnVPO_5$ contained about 5 wt% of $Sn_3V_2(PO_4)_4$ [4]. Single crystals for structure analysis were obtained by annealing the $SnVPO_5$ powder sample at 750 °C in evacuated and sealed quartz ampoule followed by slow cooling down to room temperature. The single phase SnP_2O_7 was synthesized as described in [5]. V_2O_3 was obtained from V_2O_5 by reduction in hydrogen flow.

X-ray powder diffraction data were collected on a RINT2000 powder diffractometer (θ–θ geometry, Cu$K\alpha$-radiation, scintillation counter). The single crystal data collection was performed on a CAD-4 diffractometer. Crystal structure refinement was carried out by the JANA2000 program package [6]. Further details of the crystal structure investigation can be obtained from the Fachinformationszentrum Karlsruhe, 76344 Eggenstein-Leopoldshafen, Germany (fax: (49) 7247-808-666; e-mail: crysdata@fiz.karlsruhe.de) on quoting the depository number CSD 415445.

The localization of tin atom lone pair was visualized using electron localization function (ELF) [7]. SCF calculation was performed by TB-LMTO-ASA program package [8] using Barth–Hedin exchange-correlation potential for 36k-points in the irreducible Brillouin zone. The ELF distribution was obtained using the intrinsic program procedure.

Magnetic data were collected on a commercial SQUID magnetometer MPMS-XL, Quantum Design. There was no significant difference between the data obtained under zero-field cooling and field cooling conditions. We define, in this paper, the magnetic susceptibility χ simply as the magnetization M divided by the magnetic field H.

3. Results and discussion

3.1. Crystal structure

$SnVPO_5$ single crystal was indexed in a triclinic cell with the lattice parameters of $a = 5.2633(4)$ Å, $b = 6.5252(9)$ Å, $c = 6.8785(10)$ Å, $\alpha = 113.283(11)^\circ$, $\beta = 108.037(9)^\circ$, $\gamma = 94.603(9)^\circ$, $Z = 2$. The structure was successfully solved in the space group P-1. The position of the tin atom was obtained by direct methods, then the coordinates of the V, P and O atoms were determined by sequential series of Fourier and difference Fourier synthesis. The final refinement was carried out in an anisotropic approximation for displacement parameters for all atoms and resulted in R/R_w values of 0.024/0.027. Experimental and crystallographic data are listed in Table 1. Atomic coordinates and main interatomic distances are given in Tables 2 and 3, respectively.

Table 1
Data collection and structural parameters for $SnVPO_5$

Formula	$SnVPO_5$
Temperature (K)	293
Formula weight	280.6
Crystal system and Space group (No.)	Triclinic P-1 (2)
a (Å)	5.2633(4)
b (Å)	6.5252(9)
c (Å)	6.8785(10)
α (°)	113.283(11)
β (°)	108.037(9)
γ (°)	94.603(9)
V (Å^3)	200.70(5)
Z	2
D_{calc} (g/cm^3)	4.642
Radiation, wavelength (Å)	Mo$K\alpha$, 0.71073
μ (/cm)	8.851
Color	Brown
Diffractometer	CAD4
Crystal size (mm^3)	$0.1 \times 0.12 \times 0.07$
No. of independent reflection ($I \geqslant 3\sigma$)	2345
Range of h, k, l	$-3 \rightarrow h \rightarrow 6$ $-8 \rightarrow k \rightarrow 8$ $-9 \rightarrow l \rightarrow 9$
Refinement	On F
Program used	JANA2000
$R/R_w(I > 3\sigma(I))$ or R_P/R_{wP}	0.024/0.027
No. of refined parameters	73
Weighting scheme $(\Delta/\sigma)_{max}$	Unit
$\Delta\rho_{max}$ (e/Å^3) positive/negative	1.15/−1.77

Table 2
Atomic coordinates and displacement parameters for $SnVPO_5$

Atom	x	y	z	U
Sn	0.58924(4)	0.77816(3)	0.53898(3)	0.01258(5)
V	0.84088(7)	0.36631(6)	0.23953(6)	0.00510(9)
P	0.82573(12)	0.80830(9)	0.10490(10)	0.00554(15)
O(1)	0.2227(3)	0.4974(3)	0.4616(3)	0.0069(4)
O(2)	0.5703(3)	0.7582(3)	0.8925(3)	0.0093(5)
O(3)	0.0711(4)	0.7508(3)	0.0364(3)	0.0109(5)
O(4)	0.7677(4)	0.6648(3)	0.2244(3)	0.0091(5)
O(5)	0.8966(4)	0.0659(3)	0.2706(3)	0.0098(5)

Table 3
Main interatomic distances (Å) and angles (°) in the $SnVPO_5$ structure

Sn–O(1)	2.3211(18)	V–O(1)	1.9732(15)
Sn–O(1)	2.1205(19)	V–O(1)	2.039(2)
Sn–O(2)	2.518(2)	V–O(2)	2.0214(17)
Sn–O(4)	2.493(2)	V–O(4)	2.0527(17)
Sn–O(5)	2.5267(18)	V–O(5)	2.088(2)
P–O(2)	1.5441(17)	V–O(3)	1.964(2)
P–O(3)	1.532(2)	V–V	3.0921(5)
P–O(4)	1.538(3)	O(1)–V–O(1)	79.18(7)
P–O(5)	1.5443(16)	O(2)–V–O(3)	101.41(8)

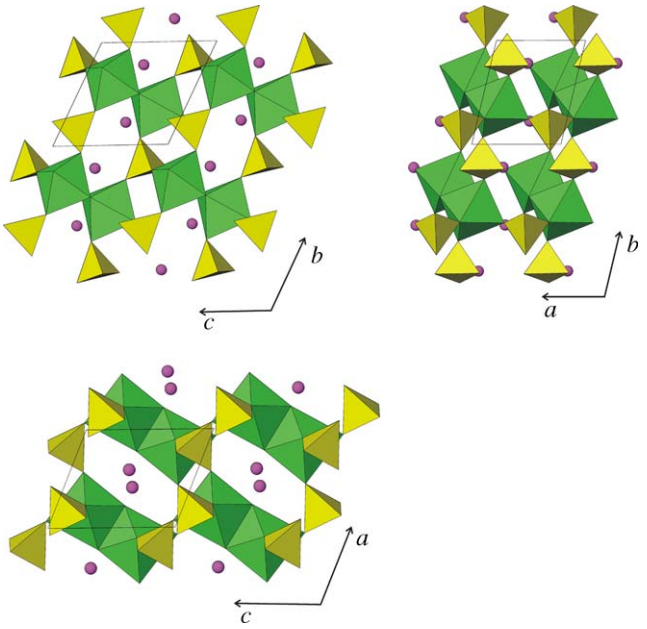

Fig. 1. Three projections of the $SnVPO_5$ crystal structure.

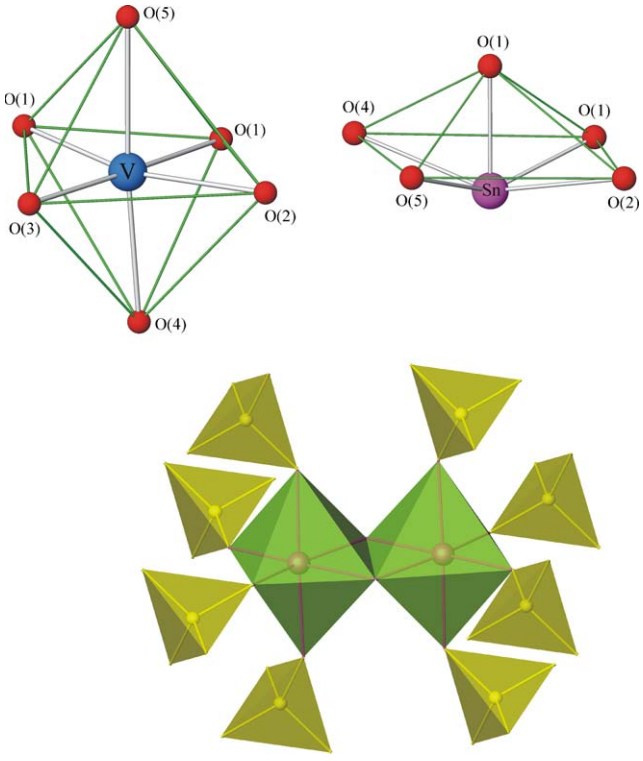

Fig. 2. Coordination polyhedra and V_2O_{10} unit in the $SnVPO_5$ structure.

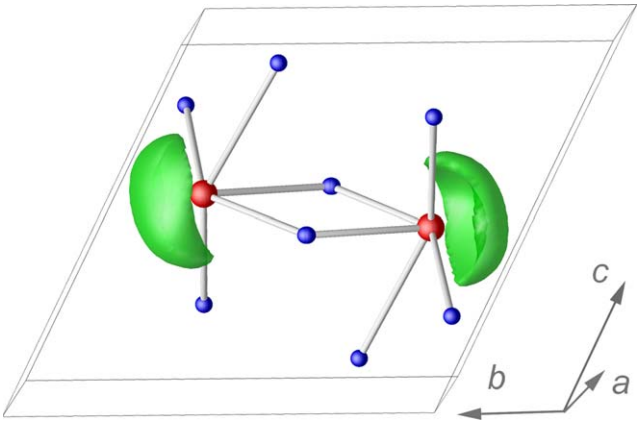

Fig. 3. Valence electrons ELF isosurface ($\eta = 0.85$) around Sn atom.

Three projections of the $SnVPO_5$ crystal structure are shown in Fig. 1. The structure contains V_2O_{10} dimers linked by PO_4 tetrahedra into three-dimensional (3-D) framework. The vanadium atom has an octahedral coordination and its oxidation state calculated from the formula is +3. The bond valence sum (BVS) calculation confirmed the oxidation state giving the value of +2.83. The tin atom coordinates five oxygen atoms and its oxidation state is +2.

The V–O distances in the VO_6 octahedra vary in the range of 1.964(2)–2.088(2) Å. The octahedron is noticeably distorted as it is seen from the values of the O–V–O angles (Table 3). Two octahedra share their O(1)–O(1) edge resulting in the V_2O_{10} dimers with the separation between vanadium atoms of 3.0921(5) Å. Four other corners of each octahedra in the V_2O_{10} unit are shared with the almost regular PO_4 tetrahedra (Fig. 2). Since the O(1) atoms belong only to the octahedra and are not linked with the phosphate groups, two systems of the mutually perpendicular channels are running along the *a*- and *b*-axis. The tin atoms having square pyramidal coordination are situated in these channels. Tin atom is slightly shifted off the base plane towards the direction opposite to the O(1) atom (Fig. 2). There are three long Sn–O distances about 2.50 Å, one medium 2.3211(18) Å and one short 2.1205(19) Å. Two neighboring SnO_5 pyramids share their O(1)–O(1) edges resulting in the Sn–Sn separation of 3.3020(3) Å. The shortest distance between tin atoms in the neighboring pair is slightly longer (3.4569(3) Å). The tin atom has a sterically active lone electron pair and, therefore, its coordination should be considered as the SnO_5E octahedron, where E represents the lone pair. The ELF calculation was performed for visualization of the lone pair. Fig. 3 displays the orientation of the lone pairs belonging to the neighboring tin atoms. They are directed oppositely and oriented toward the O(1) atom.

Both vanadium dimer and tin five-fold coordination in $SnVPO_5$ occurs rather rarely in inorganic structures. In the $KV_4P_7O_{24}$ phosphate the V_2O_{10} dimers are linked into 3-D framework by both phosphate and pyrophosphate groups [9]. In $Cd_3V_4(PO_4)_6$ [10] and $CaV_2(PO_4)_2(HPO_4)$ [11] these groups are arranged in layers. $SnVPO_5$ is the next example of the structure

containing isolated $V_2^{3+}O_{10}$ groups but the motif of the V_2O_{10} dimers connection is different. Besides, no magnetic measurements were performed for potassium, cadmium and calcium compounds. Among mentioned crystal structures the V–V separation in $SnVPO_5$ is the shortest (3.092 Å) in comparison with Ca-contained (3.211 Å), Cd-contained (3.200 Å) and K-contained (3.199, 3.211 and 3.143 Å) structures.

The five-fold coordination for tin(II) atom also is not a common case. Such coordination, for instance, was found in $SnHPO_4$ [12]. The Sn–O distances in the tin(II) hydrophosphate structure are close to those in the $SnVPO_5$ one, with the shortest separation to the apical oxygen atom. In both structures the lone pairs of tin atoms are directed toward each other. One should note that the AO_5E coordination is more typical for other elements with the lone electron pair such as Pb^{2+} or Sb^{3+} (see for example, [13]). However, this fact may be explained by the relatively small number of the known Sn(II) oxide structures.

Recently the crystal structure and magnetic properties of the $BiCoPO_5$ oxide were reported [14,15]. The structural motif of this compound is similar to that of $SnVPO_5$. Co_2O_{10} dimers are connected by phosphate groups via eight of ten oxygen atoms and form 3-D framework. Note, that Bi^{3+} cation also has lone pair and its position was localized in [19]. Nevertheless, mutual orientation of the M_2O_{10} dimers in these structures differs.

3.2. Magnetic properties

The magnetic susceptibility for $SnVPO_5$ shows a broad maximum at 22 K as seen in Fig. 4(a). It is extrapolated to be about 9×10^{-3} emu/mol at 0 K after extraction of low temperature upturn which is probably due to magnetic impurities and/or crystal defects. (One should note that $Sn_3V_2(PO_4)_4$ [4] compound exhibits paramagnetic $\chi(T)$ dependence.) Thus, the ground state of the compound is expected to be not a spin-singlet state but an antiferromagentically ordered one, and the broad maximum is caused by a short-range order. Indeed, a kink in the susceptibility above 2 T (Fig. 4(b)) appears probably due to the antiferromagnetic transition. Almost constant behavior below the transition temperature T_N suggests that the spin–flop transition field is below 2 T. On the other hand, no sign of magnetic transition is seen in the susceptibility curves below 1 T. It may be explained by a very small drop of the susceptibility below the spin–flop transition field owing to well-developed short-range order. No clear anomaly was observed also by the specific heat measurement at 0 T.

Fig. 5 shows magnetization process at 2 K, which is convex upward below 2.2 T and downward above the field as clearly seen in the slope of the magnetization

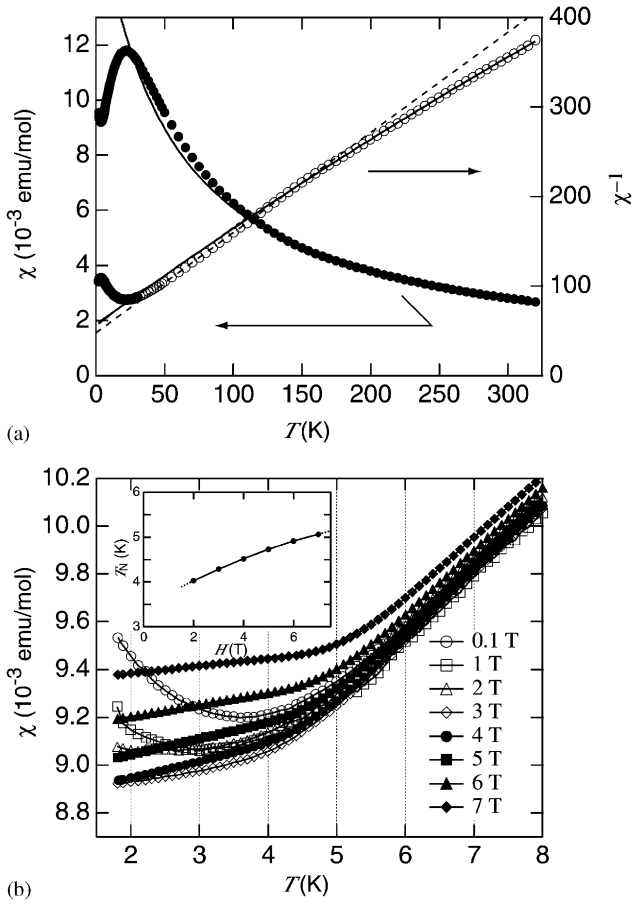

Fig. 4. (a) Magnetic susceptibility measured at 0.1 T and its reciprocal susceptibility. The solid and broken lines are the fit curve by the Eq. (1) and guide to eyes, respectively. (b) Magnetic susceptibility measured at various fields. The inset shows field dependence of T_N.

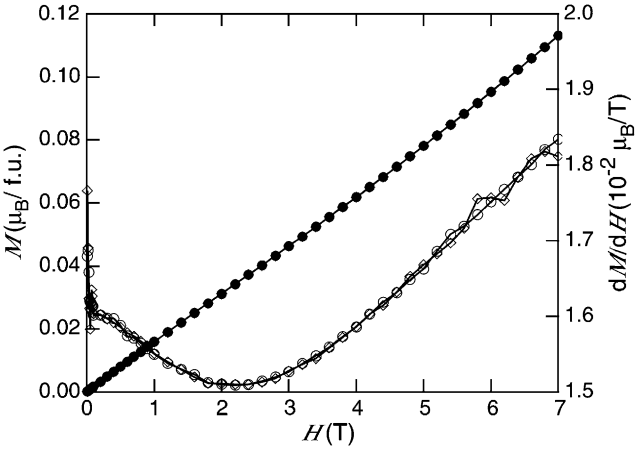

Fig. 5. Magnetization process at 2 K (full markers) and the differentiated magnetization curve (open markers). The data indicated by the circular and square markers were collected with increasing and decreasing field, respectively.

curve. The lower field behavior obeys the Brillouin function caused by extrinsic components, such as the impurities and the defects. On the other hand, the

magnetization curve above 2.2 T could be attributed to low-dimensional spin correlations which are suggested also by the broad maximum of the susceptibility. In general, such a behavior implies a low-dimensional spin system (see for example, [16]).

Let us consider the possible origin of low-dimensional spin correlations. As mentioned above, the compound contains the V_2O_{10} dimer units which are connected with each other by the PO_4 tetrahedra. It is known that PO_4 tetrahedra can mediate large spin-interactions [17]. The connection forms ladders of V sites along the *a*- and *b*-axis, and so, a slab-like structure is recognized parallel to the *ab* plane. On the other hand, the V^{3+} ion in a slab is connected with four V^{3+} ions in the adjacent slab via PO_4 tetrahedra, and the V sites form a pyramidal configuration. The geometrical spin-frustration of the pyramid could effectively reduce the interslab interaction. Thus, it is most likely that 2-D spin-correlation in a slab is dominant, because spin-dimers or a ladder is expected to have a spin-singlet ground state. In other words, the spin correlations in the compound can be regarded as a dimer array on a square lattice (DASL). The DASL model has been theoretically expected to show superconductivity with high transition temperature [18]. Until now, only $BaCuSi_2O_6$ has been known to have the structure applicable to the DASL model [19]. However, the intradimer interaction in $BaCuSi_2O_6$ is too strong compared with the interdimer interactions. The latter means that the compound is the almost isolated dimer system rather than the DASL system. Thus, our compound may be the first example of the DASC model with large enough interdimer interactions, although the square lattice is distorted.

We will give comments on anomalous behavior of the field dependence of T_N and the susceptibility at high temperature region. The T_N was estimated from each susceptibility curve as a crossing point of two linear functions obtained by fitting the data below 3 K and between 5.5 and 6.5 K. As seen in the inset of Fig. 4(b), it increases with increasing field, at least, up to 7 T. This seems atypical since T_N of usual antiferromagnetic compounds can increase only in a small field due to suppression of quantum fluctuations by the field. Thus, the compound very likely has extremely strong quantum fluctuations.

The bending behavior appears around 160 K in the reciprocal susceptibility as seen in Fig. 4(a). Such a behavior is reproducible and observed at other fields. One may think that it might be due to a large Van-Vleck term. In such a case, the susceptibility should be expressed by the equation:

$$\chi = C/(T-\theta) + \chi_0 \quad (C: \text{Curie constant}, \theta: \text{Weiss temperature}, \text{and } \chi_0: \text{constant term}). \tag{1}$$

However, the fit curve by the equation for the data between 200 and 320 K deviates from the data around 160 K and indicates the bending is not due to the constant term. Moreover, the kink was seen in the differentiated susceptibilities for all the fields, although they should not depend on the constant term because of $d\chi/dT = -C/(T-\theta)^2$. Thus, a certain anomaly clearly occurs around 160 K. The parameters obtained by the fit were $C = 0.855$ emu/mol, $\theta = -49.5$ K and $\chi_0 = 3.64 \times 10^{-4}$ emu/mol. Note, that the effective moment calculated from the *C*-value is $\mu_{eff} = 2.61\,\mu_B$, which is only 92.4% of the theoretical value of $2.83\,\mu_B$ assuming $g = 2$ and $S = 1$. Since the effective *g*-value is normally more than 2, this suggests that strong quantum fluctuations may reduce the size of the effective moment. We point out that the Curie–Weiss fit may not be applicable to these data since the Curie constant exhibits relatively large field dependence and changes from 0.735 to 0.855 emu/mol. The detailed experiments such as electron spin resonance, are in progress to clarify microscopic origins of these anomalous behaviors.

One should note that inverse magnetic susceptibility data for $BiNi_{1-x}Co_xPO_5$ solid solution presented in [15] demonstrate the behavior similar to that for $SnVPO_5$ (Fig. 4a) with T_N around 20 K. The bend at 80 K resembling to a kink observed at 160 K for $SnVPO_5$ is also well seen. However, no detailed investigation or explanation of the magnetic properties for $BiNi_{1-x}Co_xPO_5$ was done.

4. Conclusion

The crystal structure of the new tin(II) vanadium (III) phosphate $SnVPO_5$ contains V_2O_{10} dimers linked by phosphate tetrahedra. The tin atom has a square pyramidal coordination due to the presence of a sterically active lone pair. The magnetic susceptibility demonstrates a broad maximum at 22 K and the magnetization curve at 2 K shows a non-linear increase due to low-dimensional spin correlations. The magnetic ground state is the antiferromagnetically ordered one. We pointed out that the magnetism of the compound could be understood by interacting spin-dimers on a distorted square lattice. Strong quantum fluctuations were suggested by an unusual field dependence of the transition temperature and the value of a Curie constant, which is unexpectedly lower than the theoretical one.

Acknowledgment

Authors are grateful to RFBR (Grant 04-03-32787) and ICDD (Grant-in-Aid APS91-05) for financial

support and P. Chizhov for ELF calculations. R. Sh. is grateful to NIMS for his stay there.

References

[1] A. Leclaire, J. Chardon, A. Grandin, M.M. Borel, B. Raveau, J. Solid State Chem. 108 (1994) 291–298.
[2] S. Boudin, A. Grandin, A. Leclaire, M.M. Borel, B. Raveau, J. Mater. Chem. 4 (12) (1994) 1889–1892.
[3] R.V. Shpanchenko, O.A. Lapshina, E.V. Antipov, J. Hadermann, E.E. Kaul, C. Geibel, Mater. Res. Bull. 40 (9) (2005) 1569–1576.
[4] R.V. Shpanchenko, A.S. Mitiaev, V.V. Chernaya, E.V. Antipov, to be published.
[5] R.K.B. Gover, N.D. Withers, S. Allen, R.L. Withers, J.S.O. Evans, J. Solid State Chem. 166 (2002) 42–48.
[6] V. Petriček, M. Dusek, JANA2000, Institute of Physics, Prague, Czech Republic, 2000.
[7] A. Savin, O. Jepsen, J. Flad, O.K. Andersen, H. Preuss, H.G. von Schnering, Ang. Chem. Int. Ed. Engl. 31 (1992) 187–188.
[8] G. Krier, O. Jepsen, A. Burkhart, O.K. Andersen, The TB-LMTO-ASA program, Stuttgart, 1995.
[9] L. Benhamada, A. Grandin, M.M. Borel, A. Leclaire, B. Raveau, J. Solid State Chem. 104 (1993) 193–201.
[10] S. Boudin, A. Grandin, M.M. Borel, A. Leclaire, B. Raveau, J. Solid State Chem. 110 (1994) 43–49.
[11] K.-H. Lii, Dalton Trans. 1994 (1994) 931–935.
[12] (a) A.F. Berndt, R. Lamberg, Acta Crystallogr. B 27 (1971) 1092–1094;
(b) L.W. Schroeder, E. Prince, Acta Crystallogr. B 32 (1976) 3309–3311;
(c) R.C. McDonald, K. Eriks, Inorg. Chem. 19 (1980) 1237–1241.
[13] P.S. Halasyamani, Chem. Mater. 16 (19) (2004) 3586–3592.
[14] M. Ketatni, F. Abraham, O. Mentre, Solid State Sci. 1 (1999) 449–460.
[15] S. Nadir, J.S. Swinnea, H. Steinfink, J. Solid State Chem. 148 (1999) 295–301.
[16] J.C. Bonner, M.E. Fisher, Phys. Rev. 135 (1964) A640.
[17] D. Beltrán-Porter, P. Amorós, R. Ibáñez, E. Martínez, A. Beltrán-Porter, A. Le Bail, G. Ferey, G. Villeneuve, Solid State Ion. 32–33 (1989) 57.
[18] K. Kuroki, T. Kimura, R. Arita, Phys. Rev. B 66 (2002) 184508.
[19] Y. Sasago, K. Uchinokura, A. Zheludev, G. Shirane, Phys. Rev. B 55 (1997) 8357.